

Effect of ribs on torque in bending of rebars

HIGAKI Satoshi^{1,a*}, NAITO Haruto^{2,b}, GO Tomoki^{2,c},
SASADA Masahiro^{2,d} and TANAKA Tatsuya^{2,e}

¹Toyo Kensetsu Kohki CO., LTD. 4-15, 2-chome, Sangenya Higashi, Taisho-ku, Osaka-city, Osaka, Japan

²Faculty of Science and Engineering, Department of Mechanical Engineering, Doshisha University, Miyakodani1-3, Tatara, Kyotanabe-City, Kyoto, Japan

^as_higaki@toyokensetsukohki.co.jp, ^bcguf4065@mail4.doshisha.ac.jp,

^cctwh0505@mail4.doshisha.ac.jp, ^dmsasada@mail.doshisha.ac.jp,

^etatanaka@mail.doshisha.ac.jp

Keywords: Bending, Rebar, Torque, Finite Element Method, Deformation

Abstract. Deformed steel bars (Rebar) are bent into various shapes as construction materials and used with concrete. Bending machines are used for processing, and torque is required to bend rebars. Understanding the torque required for rebars with variable cross-sectional shape is crucial. The purpose of this study is to clarify the relationship between torque and material deformation. Rebars and round steel bars were bent using a simple bending machine. A high-speed camera was used to observe the material deformation during the bending process. Elastic-plastic finite element analysis was also conducted to evaluate the relationship between the material deformation and torque of the rebars during bending. The following conclusions were obtained. When the circular roller contacts the round steel bar and starts bending the bar, the torque increases rapidly. Subsequently, the torque does not change easily and remains constant. On the other hand, the torque of the rebar also increases rapidly when the circular roller comes into contact. Thereafter, the torque repeats increasing and decreasing. It was confirmed that the torque required to bend a rebar exceeds that required to bend a round steel bar with an outside diameter similar to the minimum outside diameter of the rebar. The fluctuation in torque during rebar bending occurs due to the bending of the smaller outside diameter section of the rebar, which is further away from the fulcrum roller toward the circular roller. This contrasts with the bending process of round steel bars, where bending primarily occurs in the area in contact with the fulcrum roller. As the bending of a rebar progresses, part of the rebar may move away from the fulcrum roller. When a section located on the rebar receiver side from the fulcrum roller moves away from the fulcrum roller, the torque required to progress the rotation angle of the circular roller was reduced. The torque required for bending rebars is found to be between the torque required for bending round steel bars of the smallest and largest diameters of rebars.

Introduction

Rebars are steel bars characterized by their surface ribs and nodes, commonly used as construction materials. To shape rebars, a bending machine is used. The bending machine used in this study consists of a fulcrum roller, a circular roller, and a rebar receiver. The rebar is bent by the rotation of the circular roller around the fulcrum roller. The circular roller pushes the rebar and bends the rebar along the fulcrum roller. It is important to clarify the torque required to rotate the circular roller to design and develop such a bending machine. Although there is no problem in designing and manufacturing bending machines based on past experience and knowledge, it is useful to determine the change in torque during the bending process in order to further advance the machine in the future.



Higaki, S [1,2] reported on the shape of deformed rebars that have undergone bending and on the displacement of deformed rebars during the bending process. In addition, there are reports [3,4] on research related to the bending of round steel bars, such as flattening control of circular rings and shape bending of steel, which are applied to circular tubes. There are reports [5] on bending moments of square and circular cross-sections, such as bending yielding of steel. For rebars, there is a study on the performance evaluation of rebars at cryogenic temperatures [6], a study on bending and tempering [7], and a study on stress distribution in the bending section of rebars [8].

The purpose of this study is to clarify the relationship between material deformation and torque variation in rebars with axially varying cross-sectional shapes. Material deformation of round steel bars and rebars was experimentally observed and elastoplastic finite element analysis was used to determine the material deformation, based on the results of the elasto-plastic analysis, the following is reported. The experimental results demonstrate a rapid increase in rebar torque upon contact with the circular roller. Subsequently, the torque fluctuates, increasing and decreasing repeatedly, without a further significant increase. The minimum value of the increase or decrease in torque of the rebar was close to the torque required to bend a round steel bar with the smallest outside diameter of the rebar. The increase from the minimum value to the maximum value in the increase and decrease of the torque of the rebar is considered to be related to the rib of the rebar making contact with the fulcrum roller. Therefore, bending of the smaller outside diameter section of the rebar, which is slightly further away from the fulcrum roller toward the circular roller, was occurred.

Finite Element Analysis conditions

Fig. 1 illustrates a schematic diagram of the bending machine used. First, the material is placed so that it contacts the fulcrum roller and rebar receiver. Subsequently, the circular roller is rotated with the center of the fulcrum roller as the rotation center to the position of $\theta_F=180^\circ$. During this time, the rebar is bent along the fulcrum roller. Elastic-plastic finite element analysis was performed using the analysis software Simufact Forming2022. Fig. 2 shows the analytical model. The analysis was performed for the case where the circular roller was rotated around the fulcrum roller up to $\theta_F=180^\circ$. Fig. 3 illustrates an enlarged view of the rebar model. A hexahedral element with a side length of 0.5 mm was used. The material was assumed to be elastoplastic. The mechanical properties of the materials considered in the analysis are listed in Table 1. The stress-strain relationship after yielding was considered as illustrated in Fig. 4, based on results obtained from tensile tests. The circular roller, fulcrum roller, and rebar receiver were assumed to be rigid bodies. Coulomb friction was considered in the contact between the rigid and elastoplastic bodies.

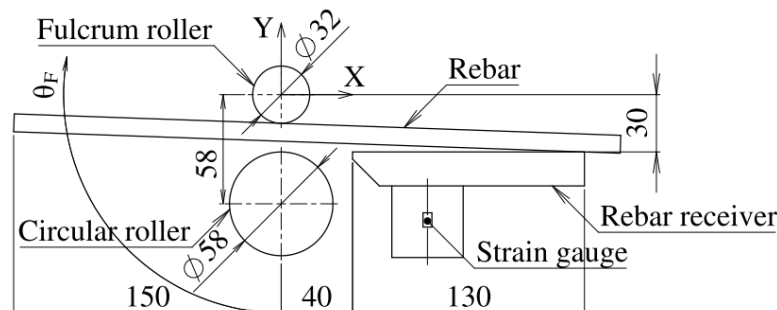


Fig. 1. Schematic diagram of the bending experiment machine.

The circular roller of the bending machine has a built-in bearing and can rotate on its own axis. FEM was also performed on a round steel bar made of the same material as rebar. The diameters of round steel bars are $\phi 10.1$ mm and $\phi 8.8$ mm. In the FEM analysis, the circular roller was set so that it could not rotate, and the coefficient of friction between the circular roller and the material was set to 0.01. In the experiment, it was observed that the nodes of the rebars were crushed and a

new surface appeared. Therefore, the coefficient of friction was set to 0.3 for the contact between the fulcrum roller and the rebar. On the other hand, the coefficient of friction between the round steel bar and the fulcrum roller was set to 0.15. The coefficient of friction between the rebar receiver and the material was also set to 0.15. The FEM analysis was performed with an increment of $\theta_F = 2.37^\circ$.

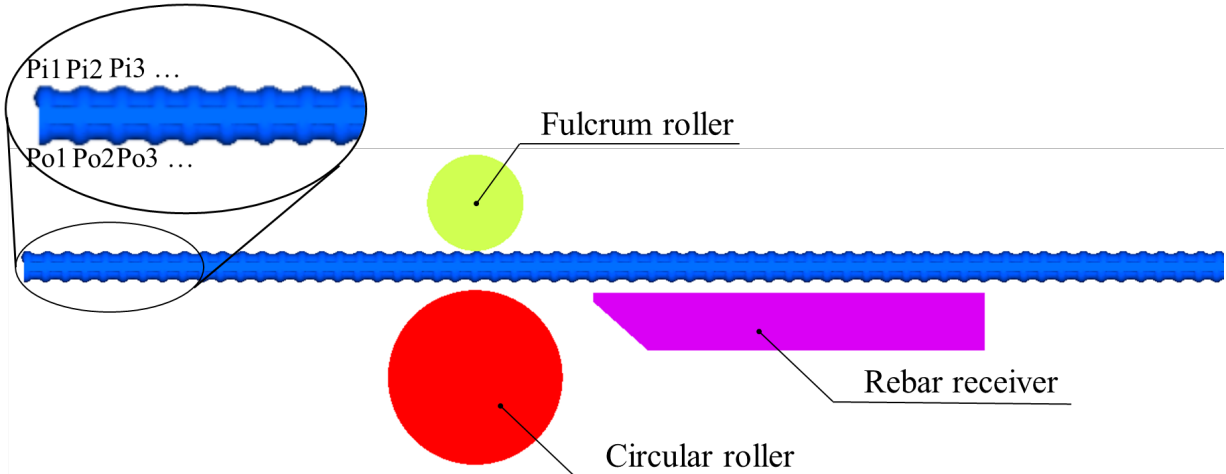


Fig. 2. Overall view of the analysis model.

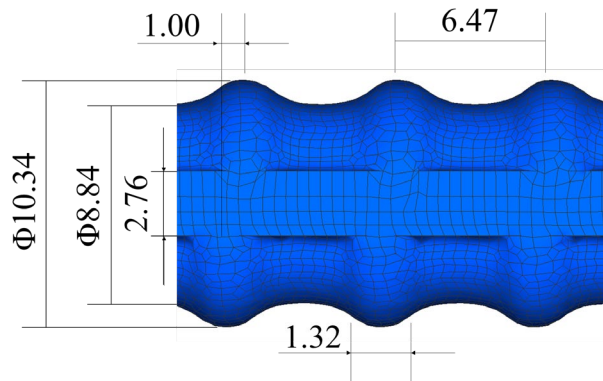


Fig. 3. Part of an analysis model of rebar.

Table 1. Mechanical properties.

Yield stress, σ (MPa)	435.9
Young's modulus, E (GPa)	205
Poisson's ratio, ν	0.3
Friction coefficient, μ	0.01, 0.15, 0.3

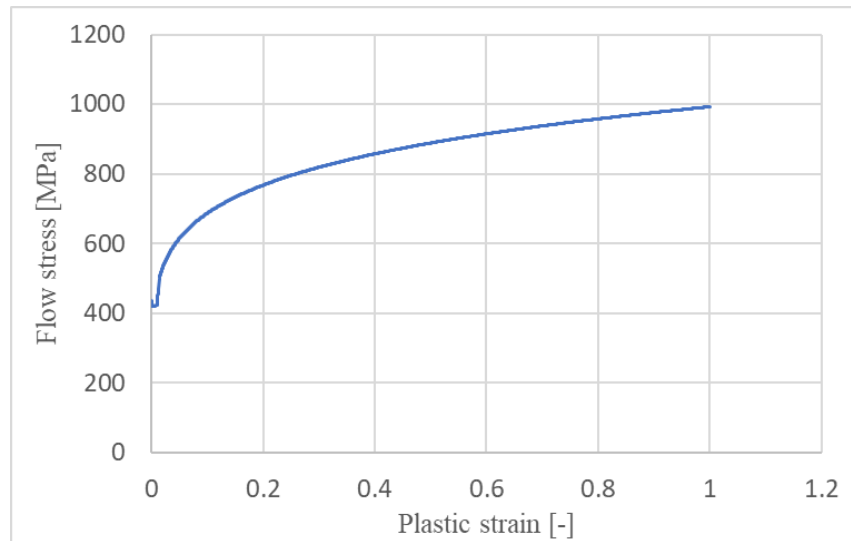
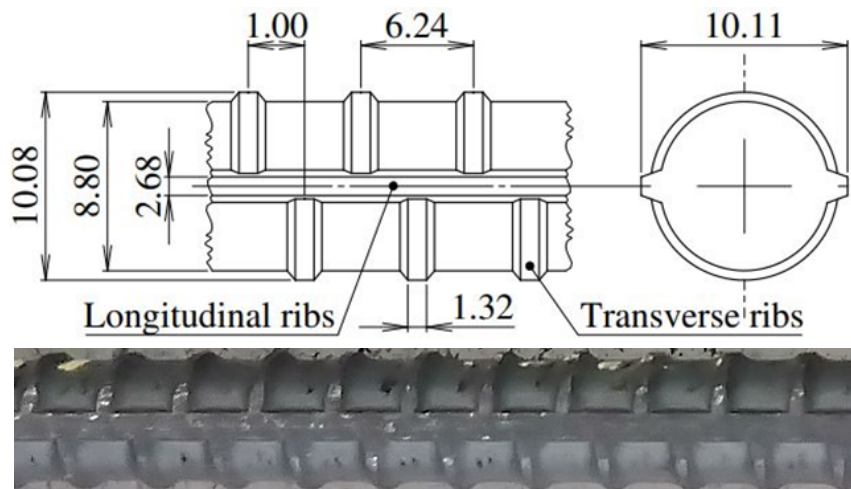


Fig. 4. True stress-plastic strain diagram.



(a) Schematic of rebar (b) Photograph of rebar

Fig. 5. Detail of rebar.

Experimental materials and conditions

Experiments were conducted to compare the results with the analytical results. Fig. 5 illustrates a schematic diagram of a rebar. The rebar is nominal D10, material SD345 (JIS G 3112), and 400 mm long. For comparison, $\phi 8.8$ and $\phi 10.1$ round steel bars machined from rebars of nominal size D13 and material SD345 were also prepared for testing and measurement. Note that the geometry of the round steel bars is the same as in the elasto-plastic finite element analysis. However, the geometry of the rebars differs from that of the elasto-plastic finite element analysis model in several areas. The maximum outside diameter of the rebar is $\phi 10.1$ mm, which is slightly different from the FEM model of rebar. The minimum outside diameter is $\phi 8.8$ mm, which is the same value as the FEM model of rebar. Therefore, the experimental results for the rebars were treated as a reference when considering the results of the elasto-plastic finite element analysis. The rotation speed was 9.8 rpm. During the bending process, a high-speed camera was placed at a distance of 290 mm vertically upward from the surface where the material was placed to capture video. The resolution was 2592×2048 pixels and the frame rate was 60 fps. Simultaneously, the torque was measured by a torque meter installed on the motor shaft of the bending machine.

Results and discussion

Material deformation during processing. Fig. 6 shows the deformed shape of a round steel bar. Fig. 7 shows the FEM results about the deformed shape of the round steel bar. At a rotation angle of $\theta_F=60^\circ$, the rebar between the fulcrum roller and rebar receiver is deflected. In the FEM result and experimental results at $\theta_F=180^\circ$, a gap was observed between the fulcrum roller and the round bar. Based on the moving image of material deformation taken during the experiment, tracking points were set on the round steel bar and trajectories were obtained using motion analysis software. Fig.8 shows the trajectory. In section P_{i20} , it can be confirmed that the displacement is in the direction away from the fulcrum roller. Thus, the analytical and experimental results are in qualitatively good agreement.

Fig. 9 shows the deformation of a rebar. Fig. 10 shows the deformation of the rebar obtained by FEM. At $\theta_F=60^\circ$, the rebar between the fulcrum roller and the rebar receiver is deformed. At $\theta_F=180^\circ$, there is a gap between the fulcrum roller and the rebar. The deformation shape at $\theta_F=180^\circ$ shows that the rebar, which has already been bent is separated from the fulcrum roller. As the rotation angle increases from $\theta_F=60^\circ$ to $\theta_F=180^\circ$, the portion bent along the fulcrum roller becomes longer. And a slight axial displacement of the rebar occurs.

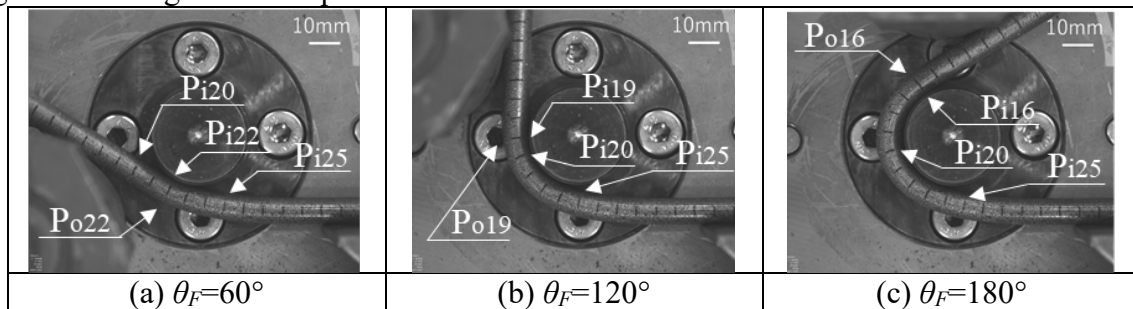


Fig. 6. Deformed shape for round steel bars with an outer diameter of 8.8 mm by EXP.

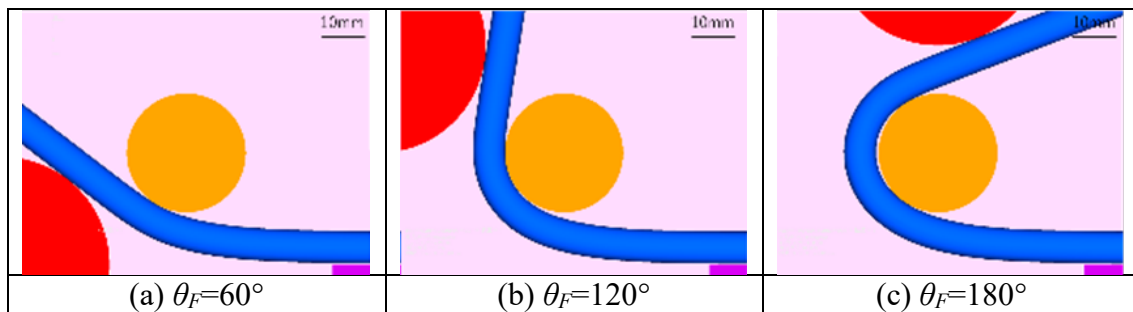


Fig. 7. Deformed shape for round steel bars with an outer diameter of 8.8 mm by FEM.

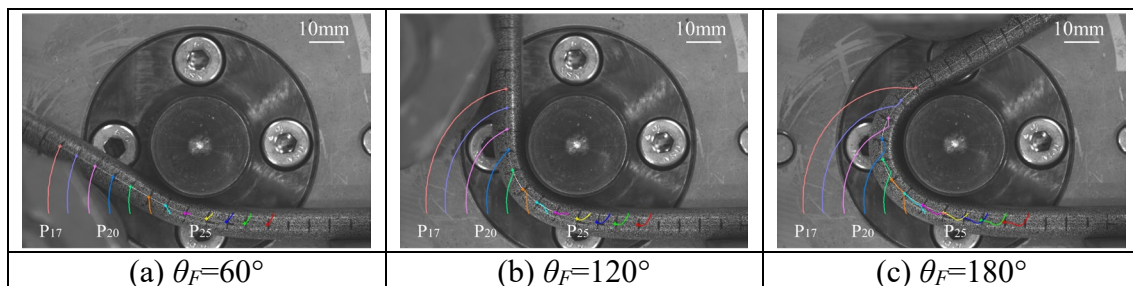


Fig. 8. Tracking point trajectory for round steel bars with an outer diameter of 8.8 mm.

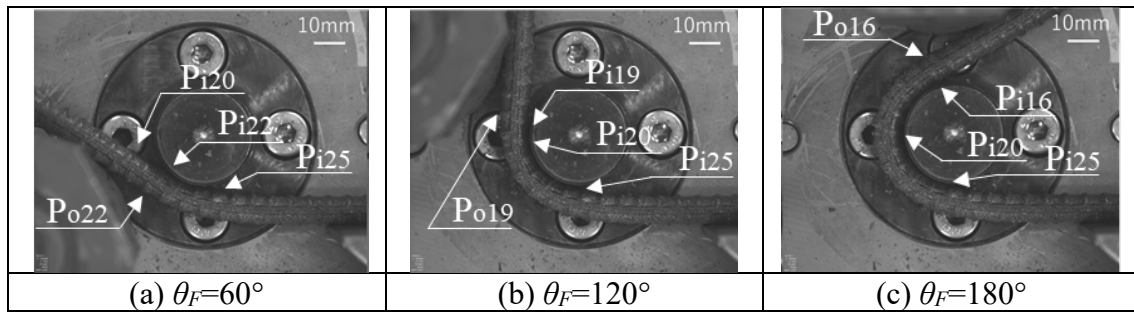


Fig. 9. Deformed shape for rebars by EXP.

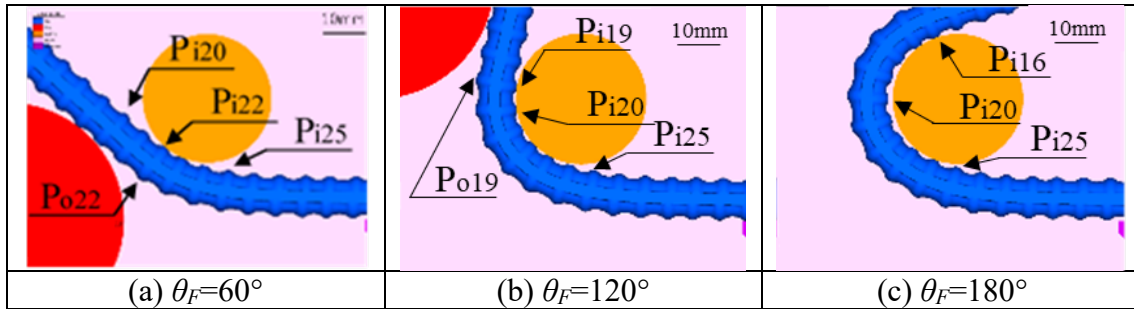


Fig. 10. Deformed shape for rebars by FEM.

Relationship between torque and rotation angle θ_F . Fig. 11 shows the change in torque measured in the experiment. Torque for rebars and round steel bars is constant after increasing. It can be seen that the processing of rebars progresses with repeated increases and decreases in torque. The magnitude of torque associated with bending rebars is less than that required to bend $\phi 10.1$ round steel bars. The minimum torque for rebars is close to that obtained by bending round steel bars with an outer diameter of $\phi 8.8$. The position of the figure center position of the cross-section of the rebar and that of the $\phi 8.8$ round steel bar are different, and since these results were obtained when the same diameter fulcrum roller was used for bending, further consideration of the handling of the figure center position is considered necessary.

Fig. 12 shows the torque variation obtained from the elastoplastic finite element analysis. The experimental and analytical results for round steel bar are in good agreement. The experimental and analytical results for rebar are also in good agreement. Therefore, we proceeded to consider torque in bending round steel bars and rebars using the results of elastoplastic finite element analysis. The torque for bending rebar can be considered with reference to the torque when bending a round steel bar whose outer diameter is the same as the minimum outer diameter of the rebar.

Increase and decrease in torque change for rebars. The material deformation was confirmed to clarify the relationship between the fluctuated torque and material deformation during the bending of rebar. In Fig. 12, one of the smallest values of torque that repeatedly increases and decreases is at $\theta_F = 110.6^\circ$. Fig. 13 shows the results obtained by FEM at $\theta_F = 110.6^\circ$. The equivalent strain, the plastic strain increment of the equivalent strain, and the region in contact with the rigid body are shown. The section numbers shown in Fig. 2 should be included in these figures to indicate the movement of sections. Rib P_{i20} is in contact with the fulcrum roller. As illustrated in Fig. 13(c), and the bending process is considered to be performed with the rib P_{i20} as the fulcrum. As can be seen from Fig. 13(b), the plastic strain increment between ribs P_{i19} and P_{i21} is large, suggesting that the bending process is progressing in this region. To compare rebars and round steel bars, Fig. 14 shows the equivalent strain, the plastic strain increment of equivalent strain, and the contact state for bending of $\phi 8.8$ round steel bar. In the case of a round steel bar, the round bar contacts the fulcrum roller over a wide area. Although not exactly the same due to the effects of the ribs, a similar trend extends over the region of greater strain for round steel bars and rebars. In other

words, at $\theta_F=110.6^\circ$, the rebar is considered to be bent along the fulcrum roller in the region where the outer diameter of the bar is small; this can be inferred from the fact that torque values similar to those of $\phi 8.8$ round steel bars were observed for rebars.

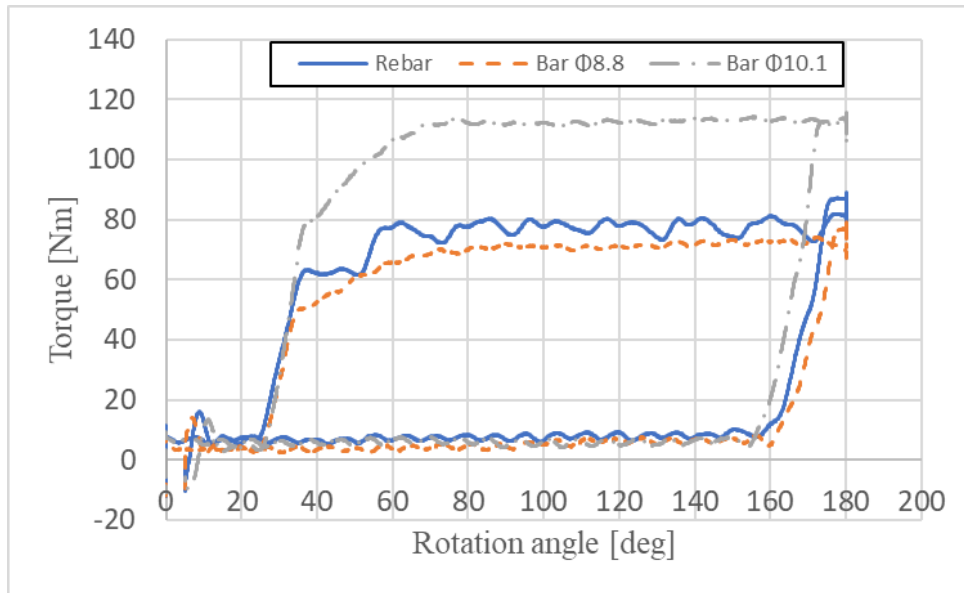


Fig. 11. Torque comparison between rebar and round steel bar in EXP.

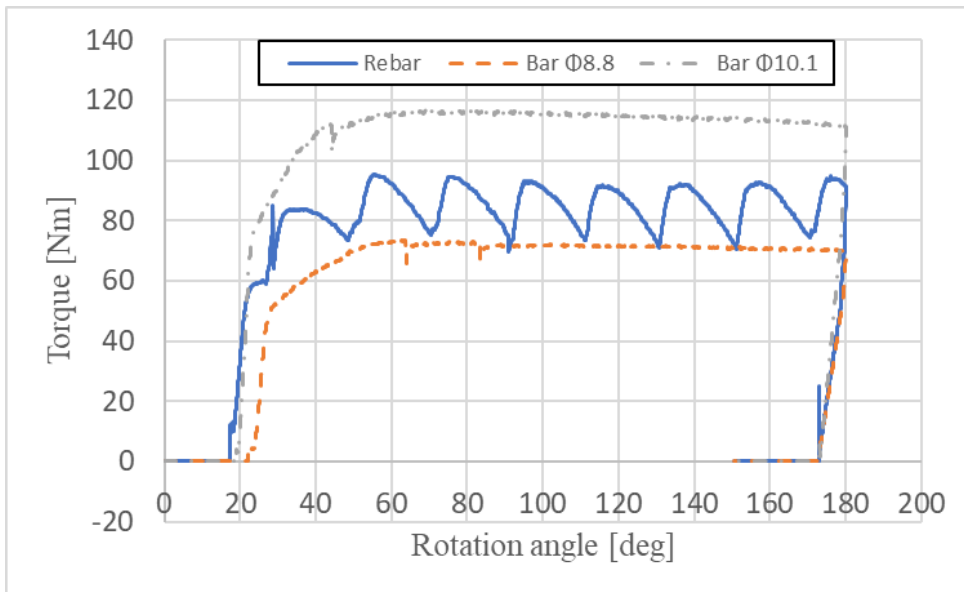


Fig. 12. Torque comparison between rebar and round steel bar in FEM.

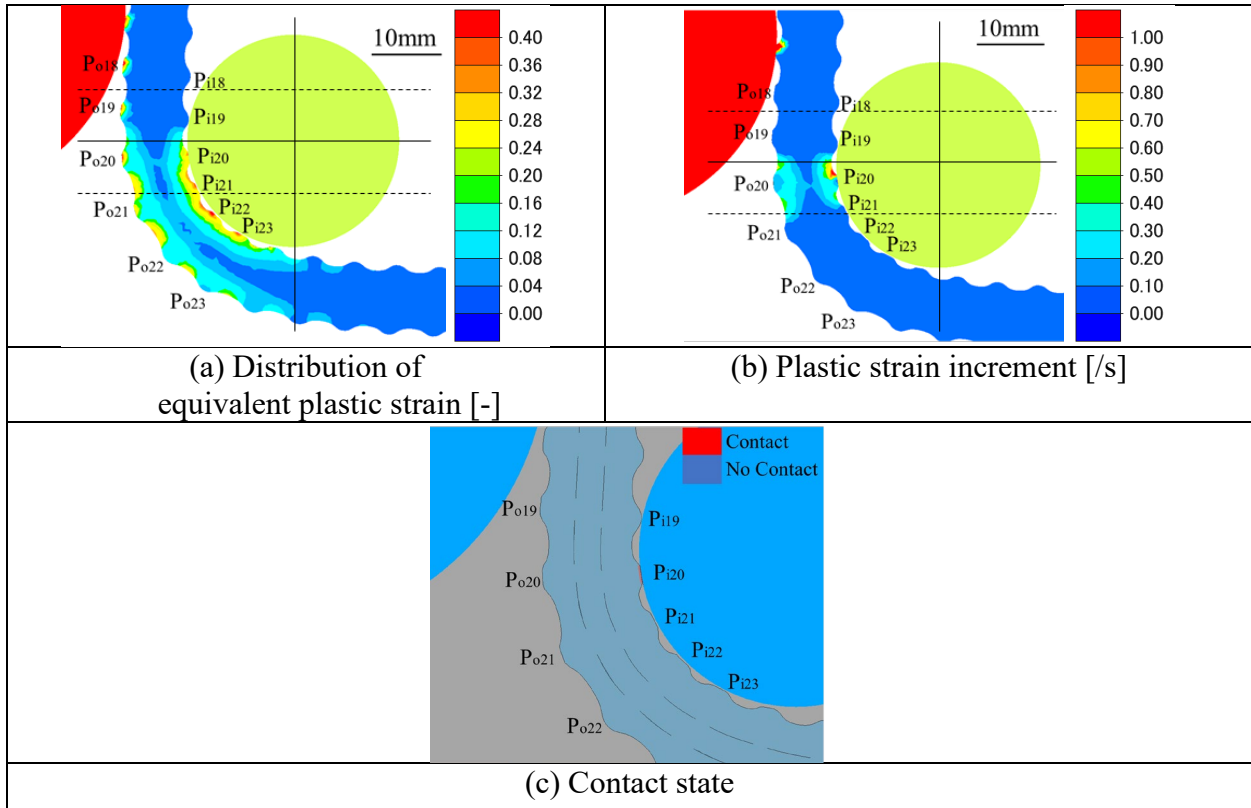


Fig. 13. Analytical results for rebar at $\theta_F=110.6^\circ$.

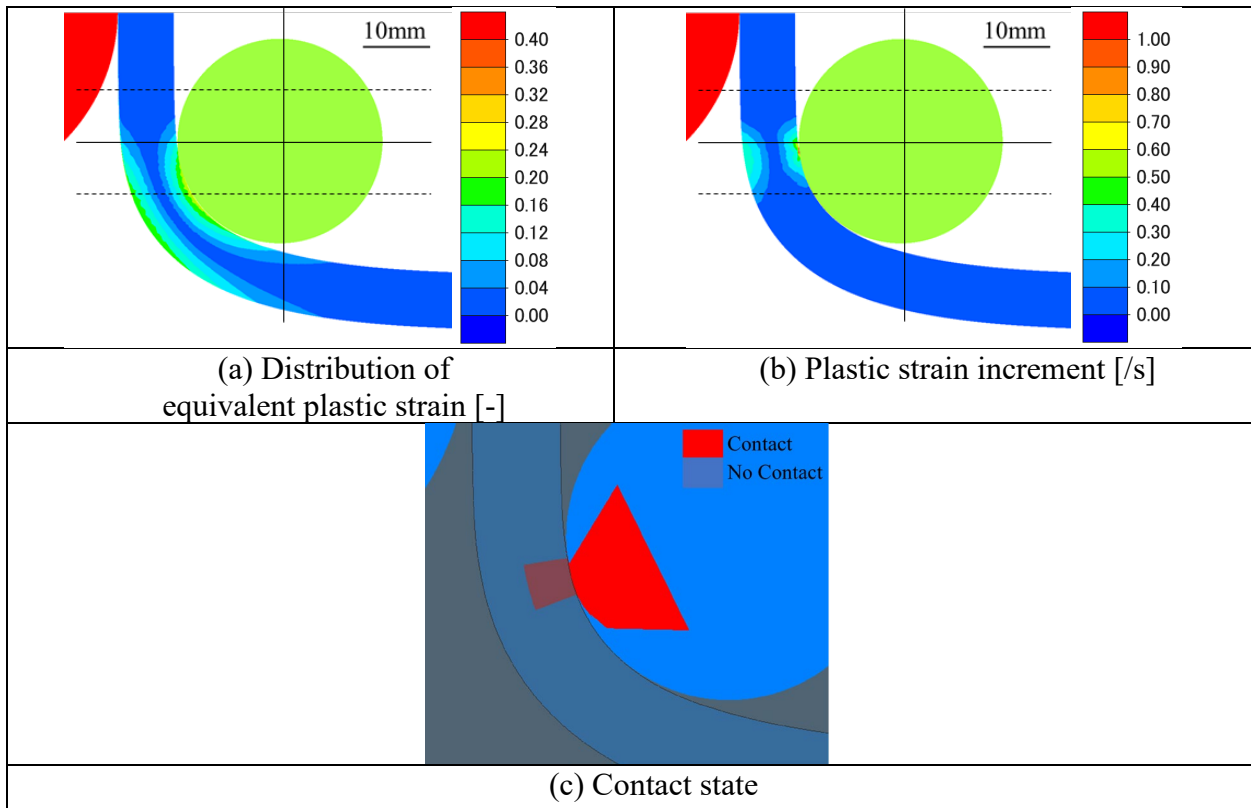


Fig. 14. Analytical results for $\phi 8.8$ round steel bar at $\theta_F=110.6^\circ$.

Consider the case where the circular roller is rotated from θ_F when the torque is minimum value, Fig. 15 shows the equivalent strain distribution at $\theta_F=112.9^\circ$ when the torque changes from minimum to maximum, at $\theta_F=117.6^\circ$ when the torque reaches its maximum value, and then at $\theta_F=131.7^\circ$ when the torque reaches its minimum value again. Fig. 16 shows the plastic strain increment at these times. Fig. 17 shows the area in contact with the rigid body. As can be seen from Fig. 16(a), for $\theta_F=112.9^\circ$, the plastic strain increment at rib P_{i19} is higher. Furthermore, as illustrated in Fig. 17(a), rib P_{i19} is in contact with the fulcrum roller. As illustrated in Fig. 16(a), at $\theta_F=112.9^\circ$, the plastic strain increment in the area with the smallest diameter between rib P_{i19} and P_{i18} begins to increase. It is thought that this area begins to bend anew as θ_F increases. As bending progresses from $\theta_F=112.9^\circ$ to $\theta_F=117.6^\circ$, the plastic strain increment between ribs P_{i19} and P_{i18} is higher. It is thought that the torque will increase as the bending process in this area progresses.

Fig. 18(b) shows the plastic strain incremental at $\theta_F=117.6^\circ$ from the FEM results for round steel bar. Comparing Fig. 16(b) and Fig. 18(b), $\theta_F=117.6^\circ$ is the same, but the position where the plastic strain increment is higher is different. In the case of round steel bars, an area with a large plastic strain increment is located near the horizontal line passing through the center of the fulcrum roller, which is represented by a solid line. In the case of rebars, on the other hand, an area with a high plastic strain increment is located closer to the circular roller than to the solid horizontal line. Thus, the rebar is bent at a location away from the circular roller due to the presence of a rib. Therefore, the external force exerted on the rebar from the circular roller to advance the bending process is greater than for round steel bars. Consequently, the torque required to rotate the circular roller is expected to increase. This difference in bending position between round steel bar and rebar is thought to be one of the reasons for the increased torque.

The torque reaches its minimum value when the circular roller is further rotated from $\theta_F=117.6^\circ$ to $\theta_F=131.7^\circ$. Fig. 17(c) shows that P_{i19} is the contact position at $\theta_F=131.7^\circ$. From Fig. 16(c), it can be observed that the plastic strain increment between the ribs P_{i19} and P_{i18} is smaller, and the plastic strain increment of the rebar on the circular roller side is smaller than that of the rib P_{i18} . The fact that the torque decreases after reaching its maximum value can be attributed in part to the separation of rib P_{i20} from the fulcrum roller. Fig. 19 shows the relationship between the displacement in the x direction and the rotation angle θ_F with respect to the position of rib P_{i20} . The angle of rotation at which rib P_{i20} contacts the fulcrum roller is between $\theta_F=110.6^\circ$ and $\theta_F=117.6^\circ$. The dotted line in the figure indicates the rotation angle at which the torque reaches its minimum value, and the solid line indicates the rotation angle at which the torque reaches its maximum value. As θ_F increases from $\theta_F=112.9^\circ$, the displacement begins to move in the negative direction of the X axis. In other words, during the bending process with rib P_{i19} as the fulcrum, rib P_{i20} moves away from the fulcrum roller. At this time torque required to advance the rotation of the circular roller is reduced. In addition, other effects on the increase or decrease in torque need to be studied in the future.

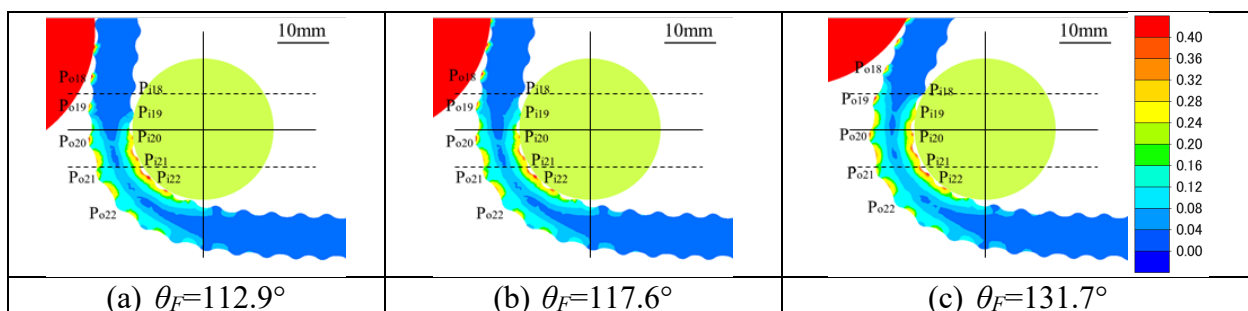


Fig. 15. Distribution of equivalent plastic strain for rebar [-].

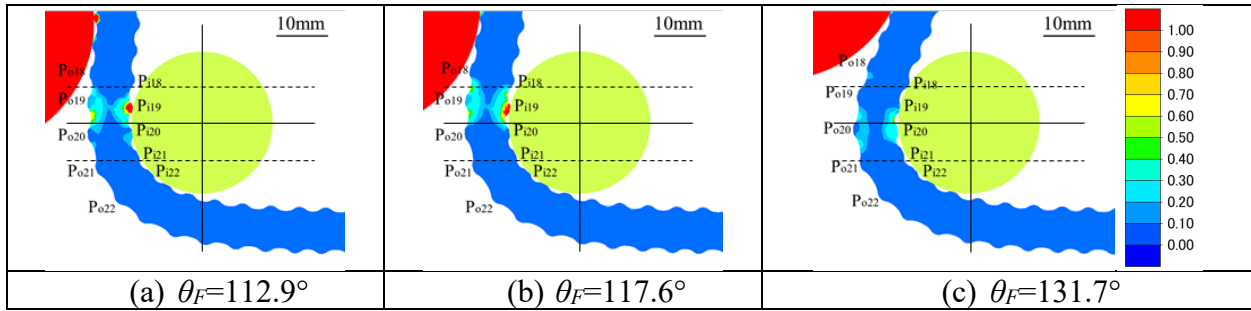


Fig. 16. plastic strain increment for rebar [1/s].

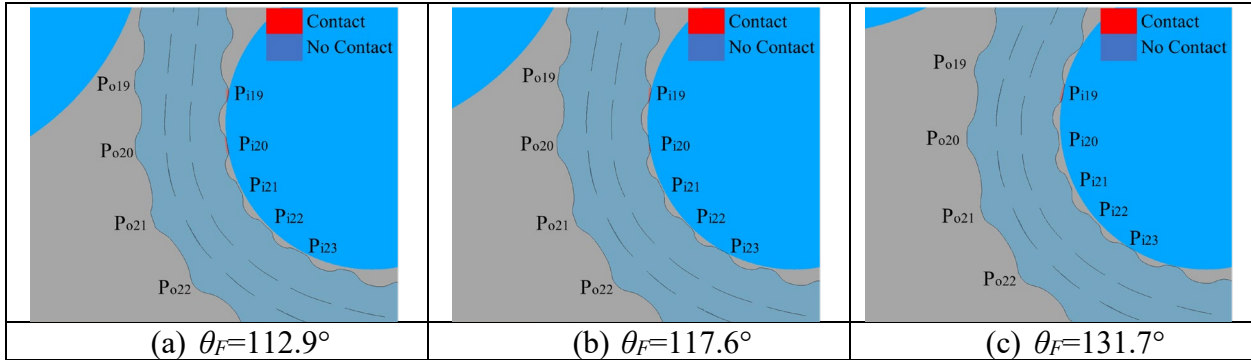


Fig. 17. Contact state between rebar and fulcrum roller.

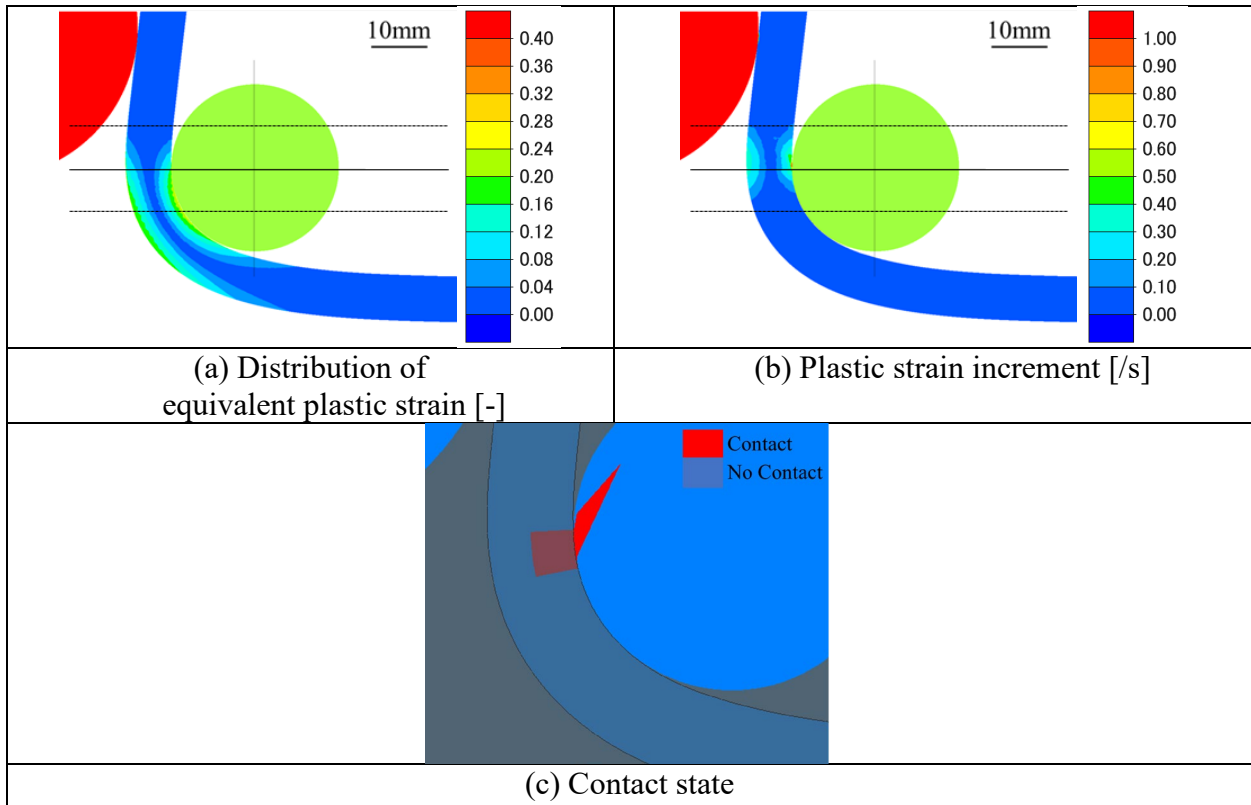


Fig. 18. FEM results for round steel bar with an outer diameter of 8.8 at $\theta_F=117.6^\circ$.

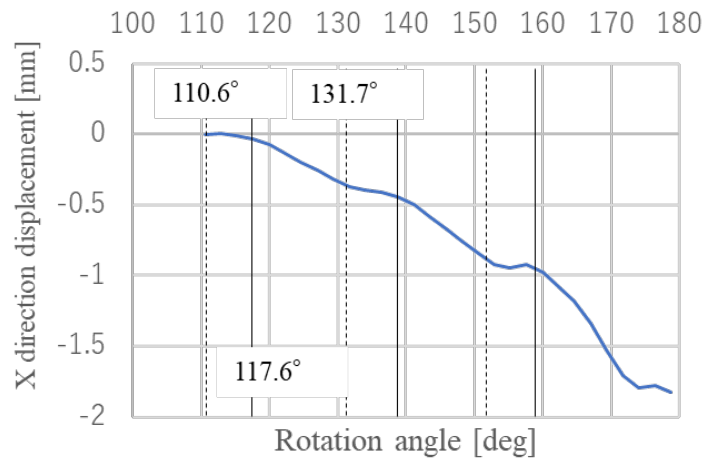


Fig. 19. X direction displacement of P_{i20} for rebar.

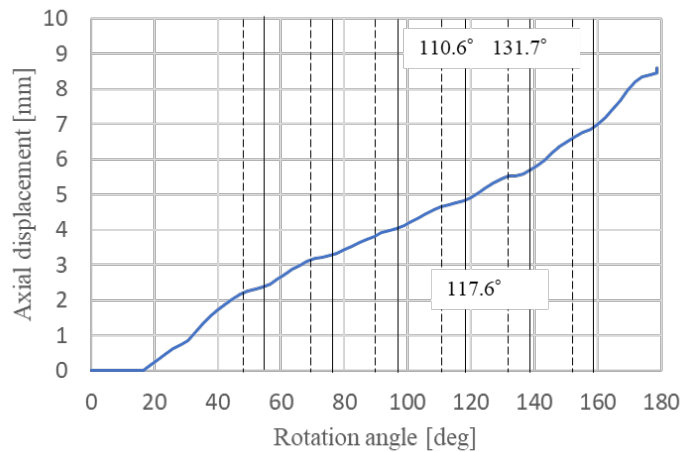


Fig. 20. Axial displacement of rebar.

Axial displacement. It was mentioned earlier that a part of the rebar separates from the fulcrum roller during the bending process. This may be related to the axial displacement of the material at the point where it contacts the rebar receiver. Fig. 20 shows the relationships between the rotation angle and axial displacement. The dotted line in the figure shows the θ_F at minimum torque and the solid line shows the θ_F at maximum torque. As the rotation angle θ_F increases, the axial displacement also increases. When the torque changes from the minimum to the maximum value, in other words, from the dotted line to the solid line, the increase in axial displacement tends to decrease. Therefore, it can be observed that this phenomenon is related to the separation of the rib from the fulcrum roller reported in section Increase and decrease in torque change for rebars.

Conclusion

To clarify the relationship between material deformation and torque during the bending of rebars, experiments and finite element analysis were conducted on D10 rebars, $\phi 8.8$ round steel bars, and $\phi 10.1$ round steel bars. As a result, the following conclusions were reached.

- (1) In the case of rebars, the torque to rotate the circular roller increases as the rotation angle increases. Furthermore, the torque does not increase significantly when the rotation angle increase. In addition, torque is fluctuating. On the other hand, for the round steel bars, the torque increases at the beginning of the process and then becomes constant. It is thought

that the bending was successively performed by rotating the circular roller for both rebars and round steel bars.

- (2) In the case of rebars, a fluctuation of torque was observed in the relationship between torque and the rotation angle. It is thought that fluctuation of torque occurred due to the effect of transverse ribs. The results of the FEM showed that the material deformation of rebars differ from that of round steel bars due to the transverse ribs. The results of FEM confirming the plastic strain increment suggest that the round steel bar is bent near the region in contact with the fulcrum roller. Compared to round steel bars, in the case of rebars, areas with large plastic strain increments are slightly deviated in the direction of the circular rollers. These differences are expected to result in a higher value of torque required for bending rebars than for round steel bars with an outer diameter equal to the minimum value of the outside diameter of the rebar.
- (3) The torque for the rebar decreases when the section closer to the rebar receiver than the section serving as the fulcrum moves away from the fulcrum roller.
- (4) It was confirmed that axial displacement occurred in the rebars as the circular roller rotated. The results of the FEM analysis demonstrated that the trends of increasing axial displacement of the rebar were related to torque fluctuation.

References

- [1] S. Higaki, T. Go, K. Mizuno, M. Sasada, T. Tanaka, Effect of Diameter of Fulcrum Roller on Shape of Rebar in Bending, Proceedings of the 14th International Conference on the Technology of Plasticity - Current Trends in the Technology of Plasticity ICTP 2023, Volume 4, 404-413.
- [2] S. Higaki, H. Nishida, Y. Koike, M. Sasada, T. Tanaka, Effect of transfer ribs on longitudinal displacement of rebars in bending, *Procedia Manuf.* 50 (2020) 253-256.
<https://doi.org/10.1016/j.promfg.2020.08.047>
- [3] K. Takahashi, T. Watanabe, T. Kuboki, M. Murata, K. Ono, K. Yano, Reduction in Flatness Using Axial Compressive Force in Rotary Draw Bending of Circular Tube, *J. Japan Soc. Tech. Plast.* 49 (2008) 896-900. <https://doi.org/10.9773/sosei.49.896>
- [4] T. Murota, J. Endow, Experimental Analysis on Plastic Deformation of Tubes in Uniform Bending, *J. Japan Soc. Tech. Plast.* 23 (1982) 343-349.
- [5] T. Nishihara, S. Taira, On the Yielding of Steel under Bending Moment (Report 2), *Trans. Japan Soc. Mech. Eng.* 18 (1952) 90-94.
- [6] T. Miura, K. Funamoto, K. Seto, Impact Resistance Ability in Bended Point of Reinforcing Bars at Very Low Temperature, *Proceedings of JSCE* 557 (1997) 15-22.
- [7] H. Okimoto, K. Turuoka, Investigation of the fracture properties of deformed bars by the bend-and-return process, *J. Struct. Constr. Eng. AIJ* 442 (1992) 33-41.
- [8] K. Sasaki, Y. Hisari, H. Igarashi, T. Miyagawa, Analysis of the strain and stress on bent section of reinforcing bar by finite element method, *Proceedings of the Japan Concrete Institute* 30 (2008) 987-992.